6-2013

Evaluating High-Resolution Aerial Photography Acquired by Unmanned Aerial Systems for Use in Mapping Everglades Wetland Plant Associations

Daniel Gann

Jennifer H. Richards

Evaluating High-Resolution Aerial Photography Acquired by Unmanned Aerial Systems for Use in Mapping Everglades Wetland Plant Associations

Synthesis Report June 2013

Daniel Gann and Jennifer Richards

CESU Agreement #W912HZ-10-2-0032

Prime Recipient Project Number: 00088394

Subaward Number: UF12261

Table of Contents

Abstract

Mapping of vegetation patterns over large extents using remote sensing methods requires field sample collections for two different purposes: (1) the establishment of plant association classification systems from samples of relative abundance estimates; and (2) training for supervised image classification and accuracy assessment of satellite data derived maps. One challenge for both procedures is the establishment of confidence in results and the analysis across multiple spatial scales. Continuous data sets that enable cross-scale studies are very time consuming and expensive to acquire and such extensive field sampling can be invasive. The use of high resolution aerial photography (hrAP) offers an alternative to extensive, invasive, field sampling and can provide large volume, spatially continuous, reference information that can meet the challenges of confidence building and multi-scale analysis.

In order for large-extent mapping projects utilizing hrAP to be successful, reliable detection of plant species is essential. Therefore, the first objective of this study was to evaluate the suitability of hrAP acquired from an UAS to support vegetation identification and detection for a specific target resolution of 2 m. We addressed the spatial accuracy of geographically referenced photography products and evaluated the adequacy of two different resolutions to detect presence and to estimate relative abundance of Everglades wetland species. The second objective was to demonstrate how spatially continuous abundance data derived from hrAP can be used to establish consistent and stable plant association classification systems in a re-sampling framework.

Recognizing plant species in the hrAP was possible in the highest resolution (1 cm) images but was limited in the medium resolution (3 cm) images. We evaluated the detection of plant species and associated morphological levels from hrAP by comparing (1) the detection agreement for class presence and (2) relative abundance estimate agreement between two interpreters. Presence/absence and relative abundance were analyzed by comparing species and morphological group profiles and summarized site profiles between interpreters. Agreement of presence and abundance between the two interpreters was very high, and confidence of species detection was very high for broadleaf species and shrubs. The recognition of short graminoid

species was almost impossible, even from the highest resolution photographs. Recognition of tree and shrubs was high at the morphological level; confidence in recognition of tree/shrub species requires more training and experience of the character classes visible in this type of aerial photography. Seasonal aspects that need to be taken into consideration during acquisition of the photographs are leaf-out and inflorescence peaks, as they can provide additional clues for identification.

When registered manually, single aerial photographs did provide accurate enough registration results and homogenous data quality throughout the image. Only radial distortion due to the nature of aerial photography needed to be considered when interpreting regions in the center or on the edges of the photographs, as the perspective changes, especially for tall emergent linear vegetation. After re-registration in alignment with a 1-ft aerial ortho-photo, the mosaic of images was used for registration of the single raw images, but quality heterogeneity across study sites due to distortions prevented us from attempting species detection from the mosaic.

In the second objective, we evaluated the effect of sampling intensity on the detection of plant associations using the visually estimated relative abundances of species from hrAP. We demonstrated how spatially continuous abundance data derived from hrAP can be used to establish consistent and stable plant association classification systems in a re-sampling framework. The hrAP was extremely useful for deriving plant association classifications, enabling estimation of class- and site-specific membership probability distributions and their associated parameters. The hrAP allowed for instantaneous visual feedback on adequacy of associations that resulted from cluster analysis. The re-sampling framework we developed enabled visual and statistical evaluation of plant associations before they are used in detection and mapping applications.

Introduction

Monitoring ecological restoration in the greater Everglades presents three major challenges: the spatial heterogeneity and complexity of the vegetation (landscape pattern); the natural intra-annual, inter-annual and decadal temporal dynamics; and the large spatial extent. Hydrologic restoration will produce changes in vegetation patterns across this large extent at different spatial and temporal scales. Therefore, we need flexible, rapid and affordable ways to monitor the patterns of change. In response to these challenges, remote sensing (RS) offers various techniques to acquire and interpret images covering entire landscapes. Remote sensing can generate information over large spatial extents without disturbing the environment and can provide greater temporal resolution than traditional sampling and mapping techniques. In order to use RS to monitor vegetation change, however, we also need rapid and affordable methods to gather ground reference information in order to train algorithms and assess the accuracy of remote sensing products.

Vegetation maps are produced at various resolutions or scales and for different purposes. For any given location the definition of the dominant plant community varies with scale and purpose of analysis. Currently, vegetation surveys and map accuracy assessment are completed with costly field sampling procedures or using helicopter surveys by specialists who visit sites and make rapid assessments of plant communities at designated sampling locations. This assessment is performed for a specific scale and for a single map only. Using high-resolution images captured by unmanned aerial systems (UAS) may offer a more affordable, reliable and repeatable assessment that can occur at various scales and that can provide historic reference data for multiple mapping efforts.

Mapping of vegetation patterns over large extents using remote sensing methods still requires field sample collections for the training process of image classification and accuracy assessment of derived maps, but especially in cases where study areas are difficult or expensive to access, high resolution aerial photography could be of great value to reduce field site visits while providing large volume reference information for continuous surfaces, as compared to point surveys of quadrat plots as are traditionally collected during field sampling campaigns.

When classifying vegetation using remotely sensed data, multiple iterations provide intermediate results that are visually evaluated and, as needed, additional training samples are added or previous samples are dropped. High-resolution aerial photography (hrAP) can be very useful for visual confidence building in the intermediate visual evaluation and for the selection of additional training samples. Once visual confidence at an acceptable accuracy is established, post-classification accuracy assessment based on some type of random sampling design is conducted. An initial post-classification accuracy assessment limited to the extent for which hrAP was acquired can confirm the visual evaluation before a larger, more expensive, and time-consuming field accuracy assessment is conducted.

The usefulness of hrAP to support detection of vegetation classes from remotely sensed satellite data depends to a large degree on the spatial accuracy of the geographically referenced aerial photographs and the detectability of vegetation classes from the photography. Highly accurate co-registration of the hrAP to field site surveys and geographically referenced satellite data is crucial. Only if the aerial photograph and the satellite data are co-registered within 0.5 times the detection resolution from the satellite data is the confidence of training sample selection for supervised classifications and support during accuracy assessment valid. A second aspect that plays a vital role in hrAP support of remote sensing is the detectability of vegetation at species level and, once vegetation associations of interest are formulated, the detection of those. Characteristics of the hrAP that are important in this process are resolution and quality consistency across the study area.

Another problem in vegetation mapping that use of hrAP may resolve is the establishment of classification schemes that are valid for multiple scales of detection and analysis. The study of plant association patterns and their dynamics across spatial scales for large spatial extents requires spatially explicit vegetation information. It is difficult to gather this type of information via field survey sampling techniques, which generally sample at a single scale. Hence, a common practice for mapping vegetation patterns over vast areas is to apply predefined vegetation classification schemes to remotely sensed data either through visual interpretation or by applying digital image processing procedures, including classification algorithms, to aerial photography or satellite data. The scale of pattern analysis and associated classification scheme definitions and the scale of detection, however, rarely coincide, and it is

common practice to make inference from small grain patterns (i.e., detection of pattern at small spatial response units, such as 1 m quadrat field surveys) to larger response units of visually interpreted photographs or pixels of a remotely sensed data set. Another common practice is to aggregate the minimum mapping unit (i.e., detection) of a vegetation map to a coarser resolution (i.e., spatial scale of analysis), combining information of multiple map objects (e.g., pixels, grid cells, or polygons) at multiples of the initial detection resolution.

For both of these practices the classification of vegetation and aggregation of vegetation classes across spatial scales is not straight forward. The effects of changes in grain size or scale on species co-occurrence patterns and vegetation classifications become apparent when rescaling vegetation surveys or maps to coarser units using different aggregation processes; different processes lead to very distinct results (Marignani et al. 2007, Rocchini 2007, Schlup and Wagner 2008, Gann et al. 2012). Spatial aggregation, therefore, can cause a disjunction between initial thematic classes of a classification scheme (i.e., plant association or community definitions) defined and detected at a fine scale (e.g., quadrat surveys) but applied and analyzed at coarser scales (O'Neill et al. 1988, Wu 1999, Francis and Klopatek 2000, Wu 2004). This disjunction can result in misleading conclusions about extant vegetation patterns and observed changes through time (Turner 1989, Lam and Quattrochi 1992, Tischendorf 2001, Ostapowicz et al. 2008, Mas et al. 2010).

Generating plant association definitions for multiple scales from a single finite random sample is not possible, since the sample always refers to the unit area that was sampled. Scaling of samples is possible of adjacent spatial units are sampled as well. Then, through the process of spatial aggregation, samples can be pooled. Field sampling of many samples with their adjacent neighboring units is very time-consuming and cumbersome. The use of hrAP can potentially overcome this limitation by providing a fine resolution data set over relatively large extents. Visual interpretation at the minimum spatial grain size (i.e., sample unit on the ground) of the hrAP can provide the base for a re-sampling framework. Incorporating re-sampling procedures at different scales and cross-validation could then allow for establishment of multi-scale, regionally valid, plant association classifications. Plant association classifications derived and validated from sets of samples collected at different grain sizes will also provide a better understanding of variability in class definitions by incorporating sampling error. This method

will allow for estimation of class stability and generality at each scale of interest, as well as across scales. Classification of unknown geographic units can then be performed with a probability estimate of class membership. The accurate classification of geographic units that have not been used in the establishment of the classification scheme is crucial in the process of general pattern recognition.

In order for large-extent mapping projects utilizing remote sensing methods to be successful, reliable detection of plant associations at different scales is essential. If community descriptions are ambiguous and detection on the ground is difficult, it will be impossible to detect these communities with remote sensing applications. Therefore, the first objective of this study was to evaluate the suitability of high resolution aerial photography acquired from an UAS to support vegetation classification and detection for a specific target resolution of 2 m, which is the spatial resolution for WorldView-2 satellite data. We addressed the spatial accuracy and adequacy of resolution to detect presence and to estimate relative abundance of Everglades wetland species. The second objective addressed the establishment and confidence building process for vegetation classification systems using the hrAP vegetation data

Objective 1: Determine spatial accuracy and adequacy of high resolution aerial photography to detect Everglades plant species and morphological vegetation groups at 2 image resolutions from a two interpreter comparison.

The first goal of this objective was to evaluate the spatial resolution and spatial accuracy of high resolution Aerial Photography (hrAP) acquired by an Unmanned Aerial System (UAS) to support vegetation mapping of plant species associations from 2 m resolution satellite data (e.g., WorldView-2). The second goal was to estimate the visual detection probability and associated accuracies for wetland species and plant morphologies (growth forms) from aerial photographs for a 2 m resolution analysis grain size. We established detection confidence by comparison of visual interpretation results of 2 interpreters. We were also interested in the change in detection confidence from geo-referenced single images when decreasing the spatial resolution (i.e., photographing from different elevations).

Methods

Aerial Photography Evaluation and Processing

In order to use this hrAP in support of the satellite remote sensing process, it was essential that the aerial photographs and field-collected reference data were geographically referenced to a spatial accuracy of within 1 m (0.5 * the grain size of the 2 m analysis resolution). The raw images we received from the US Army Corps of Engineers (ACOE) for the two study areas 'WEST' and 'EAST' were catalogued (Figure 1) based on approximate ground resolution derived from flight altitude at acquisition. The two resolution levels we established were 'high' resolution photographs acquired above 25 and below 75 meters and the second resolution acquired between 100 and 170 meters above ground (mag). Of the 2182 images that had their reference location within either of the 2 study sites, 188 were classified as 'high' resolution images (WEST = 91, EAST = 97) with an acquisition altitude of 35.7 ± 8.4mag (mean ± SD, Table 1). The remaining 1994 'medium' resolution images (WEST = 1063, EAST = 931) were acquired at an altitude of 136.1 ± 11.8 mag (Table 1). Since we had visited and collected only reference samples in study area WEST, we limited the analysis to that study area. The

methods developed in that area could be extended to the EAST region later to build confidence in the developed procedures and protocols.

We first evaluated the spatial accuracy of the medium resolution photography mosaic provided by the ACOE. The initial spatial accuracy of the geo-referenced mosaic was established from a 1-ft resolution ortho-rectified aerial photograph of 2011 (CERP). A quantitative analysis of 16 reference locations spread across the full scene indicated that the positional accuracy was not uniform across the mosaic. The shift in x and y dimensions was between 5 and 7 meters in either dimension. The directional RMSE was 2.8 m ranging from -4.3 to +0.9 m in longitudinal direction and 4.5 m with a range from -0.5 to -7.1 m in the latitudinal direction. This translates into a Euclidean distance RMSE of 5.2 ± 2 m. Hence, given our 2 m resolution grain size, we concluded that the positional accuracy of the mosaic was not acceptable to perform ground-referencing work for training and accuracy assessment of visual interpretation or the remote sensing procedure. Therefore, combining field data collected on August 15th, 2012 and March 13th, 2013 and utilizing the 2011 ortho-rectified aerial photograph, we geo-referenced the ACOE mosaic using a 2nd order polynomial with a reported model-based positional RMSE of 0.29 ± 0.13 m. Through post-rectification accuracy assessment using the same 16 reference points we used to evaluate the mosaic, we determined that the positional accuracy was improved to an overall remaining Euclidean RMSE of 0.7 m (lon = 0.5 m; lat = 0.5 m).

For the evaluation of detection probability at the highest image resolution, we selected 3 of the 91 low altitude images (Table 1); images were selected that had the highest visual variability in species presence. The 3 selected images from East to West were 20120816222532_513, 20120816222532_557, and 20120816222532_550, and were acquired at altitudes of 33.7, 34.2 and 32.2 meters above ground (mag) respectively. We geo-referenced the images (ArcGIS) using a 2nd order polynomial with a RMSE of 16.7, 12.8, and 28.5 cm respectively (Table 2), which resulted in a nominal spatial resolution of approximately 1 cm for all referenced images (Table 2; Spatial Reference Resolution). This resolution was supported by the higher nominal ground resolution calculated from the camera and acquisition specifications of the flight (Table 2; Nominal Ground Resolution). For each 1 cm resolution image we geo-referenced the corresponding lower resolution, high altitude image whose centroid was closest to the centroid of the higher resolution image (Table 2). The closest matching image for _513 was

far off its recorded image center and was, therefore, discarded. The next closest matching image was 20120815030421_285, acquired at 128.6 mag. Image 20120814230041_255 matched image _557 and was acquired at 128.2 mag. The closest image to _550 was not well-focused, and the second closest could not be well-referenced, which made the third closest image 20120814230041_719, acquired at 133.5 mag, the best option. The spatial resolution of the referenced images was approximately 3.1 cm (Table 2; Spatial Reference Resolution) when registered with a 2nd order polynomial model with RMSEs of 15.1, 26, and 28.5 cm respectively (Table 2).

Species List and Associated Morphological Groups

Based on field work in the study area, digital image pattern recognition experience and species characteristics, we established a hierarchical classification scheme with species or taxon groups at the finest level and their associated morphological growth form (morphological level) at the next higher level (Table 3). The criteria used to establish species-level categories included overall abundance in the study area (excluding rare species for lack of training opportunity), plant size, and localized density patterns. All taxa included in the list were expected to be recognizable from 1-2 cm resolution RGB aerial photographs, the highest resolution we would evaluate. If a plant was too small to be detected as an individual, but the expected growth density allowed it to be differentiated from its surrounding environment, it was included.

The species we attempted to identify were grouped into 9 **morphological groups** (Table 3). The **floating broadleaf** group included species *Nymphaea odorata, Nymphoides aquatica, Nuphar advena*; the **floating non-broadleaf** group of included the bladderworts *Utricularia foliosa* and *Utricularia purpurea*. The group of **emergent broadleaf** species was further divided into a sub-class of ferns with only *Acrostichum danaeifolium* expected to be identifiable at the species level. The other broadleaf species we attempted to identify were *Peltandra virginica, Crinum americanum, Sagittaria lancifolia, Pontederia cordata,* and *Thalia geniculata*. In the group of **short graminoid** species we included *Panicum hemitomon, Rhynchospora tracyi, Rhynchospora inundata,* and *Eleocharis* ssp. *Cladium jamaicense* and *Typha domingensis* were the only two species we differentiated in the **tall graminoid** group. **Herbaceous** vegetation was identified only at the morphological group level. **Shrub** species included *Salix caroliniana,*

Myrica cerifera, Chrysobalanus icaco, and *Cephalanthus occidentalis*, and in the **tree** group we tried to differentiate among *Annona glabra, Magnolia virginiana, Ilex cassine, Persea* ssp. and *Ficus* ssp.. Finally, P**eriphyton,** a group composed of floating and benthic periphyton, including epiphytic periphyton wrapped around stems and leaves, was also included. The complete list of all 36 classes (27 species or taxon groups, 9 morphological groups) available for visual interpretation is provided in Table 3.

Visual Photo Interpretation - Training Methods and Protocols

We generated a 2x2 m grid covering the entire study area, allowing for a 50 m buffer on all 4 sides to avoid edge effects in subsequent analysis. Grid cells that were entirely covered by the images were selected for interpretation. The 649 grid cells covering the three images were distributed over the three areas of the non-contiguous photographs, (Fig. 1) with 184, 234, and 231 cells in images 550, 513, and 557 respectively (Figures 2-513, 557, 550). For relative abundance estimates for each grid cell we divided each cell into 16 0.25 m^2 sub-grid cells (Fig 2; white grid in right zoom panels), which allowed for estimates with a precision of 6.25%. After an initial training phase, both interpreters independently assigned relative abundance estimates for each 2x2 m grid cell based on coverage of the 16 cell sub-grid estimation. For each grid cell estimated relative abundance estimates were records in a site (row) by species (columns) matrix. The visual interpretation of the 3 selected images resulted in 649 cells with abundance values ranging from 0 to 16. If a cell sum of all values was less than 16, this indicated the presence of open water or bare ground. All 649 grid cells were interpreted independently by both interpreters at the 1cm aerial photography resolution. A subset of 100 grid cells was sampled with a simple random sample without replacement (Fig. 2; blue transparent grid cells) to be also interpreted from the high altitude, 3 cm resolution images.

The interpreters were trained in the field and on screen pattern recognition. For training purposes we gathered ground reference data on August 15th, 2012, one day of aerial photography acquisition, and on March 13th, 2013. We collected 24 and 50 samples on day 1 and 2, respectively. The ground referencing survey of samples was performed using real-time kinematic (RTK) surveying equipment to establish positional accuracies of 3-5 cm. On day one we used a Trimble R6 and the Trimble network for kinematic real-time corrections, and on day

two, a Trimble R8 with the FL Department of Transportation network kinematic correction. At each sample location we recorded dominant species presence and descriptors of the site, and on day one we also recorded water depths. We also acquired 0.25 m^2 quadrat plot photographs of the site, and for a subset of sites we took panoramic photographs. All photographs are stored and linked to sample locations and data in a geographic database.

Analysis

We evaluated the detection of plant species and associated morphological levels by comparing (1) the detection agreement for class presence and (2) relative abundance estimate agreement for two interpreters. Presence/absence and relative abundance were analyzed by comparing species and morphological group profiles (columns) and summarized site profiles (rows) between interpreters. In a third analysis, we also compared high vs. medium resolution photography by interpreter, as well as the ratio of detection at species versus morphological group level and agreement for each of the interpreters.

For the presence-absence analysis we converted the relative abundance estimates to presence-absence data and converted the differences in detection by the two interpreters into an index, where 0 = not detected by either interpreter, 1 = detected by interpreter 1 only, 2 = detected by interpreter 2 only, and 3 detected by both interpreters. Adding all disagreement counts of 1 and 2 provided the site-specific presence agreement. For each cell we also calculated diversity for each interpreter, assuming that if species estimates were assigned, that a morphological assignment for the same group for the same cell was due to at least 1 unidentified other species of that group being present. Species profiles for presence agreement were generated by cross-tabulating the presence agreement index table across all sites for each species. In a similar fashion we generated the morphological site profiles and morphological group profiles across sites. We assigned presence for a morphological group if at least one species of the group had been detected or if the group was detected without species specification. Cross-tabulating the agreement index table provided the basis for calculating the species-specific presence agreement in percent. The analysis of differences in relative abundance estimates was based on difference tables generated by subtracting the estimates of interpreter 2 from those if interpreter 1.

From the index and difference tables we generated 6 parameters of agreement: (1) relative species abundance estimates and (2) relative site presence agreement across all sites (species profiles); (3) morphological group abundance and (4) presence profiles (morphological group profiles); (5) summarized site profiles of corrected differences for species level evaluation, discounting for detection at the morphological group level of one interpreter but at the species level by the other interpreter; and (6) the difference in site diversity estimates. The third analysis evaluated the ratio of detection at species to morphological group level evaluated by interpreter. The parameters of interest were agreement of class abundance estimates of the lower resolution interpretation with the higher resolution data, and the reduction of detection at the species level when compared with interpretation at the higher resolution data.

Results

Presence/Absence Species Profiles

Of the 28 species/taxa (including sub-group ferns and group periphyton) on the species list, 9 were not detected by either interpreter in any of the 649 cells. For *Nuphar advena, Acrostichum danaeifolium, Thalia geniculata and Typha domingensis,* we suspect the species were not present since detection of these species should be comparable to other broadleaf and tall graminoid plants that were detected frequently. In the case of short graminoids *Rhynchospora tracyi, Rhynchospora inundata,* and *Eleocharis* ssp., detection of individual plants was very unlikely, but detection of larger dense patches was expected, which means the species were not present, too sparse or too rare to detect. Absence of tree species *Ilex cassine* and *Ficus ssp.* was attributed either to absence in the sampled area, or to limited recognition due to interpreter inexperience. These species were most likely to be confused with *Magnolia virginiana* or *Persea* spp.

Summary statistics are provided for only those species that were actually identified at least once by either interpreter (Table 4). The range of class agreement (presence and absence) of all 19 detected species classes ranged from 89.2% for *Peltandra virginica* to 100% for *Panicum hemitomon* (Table 4, column % Agree). The most frequently-encountered classes identified at the grid cell level by both interpreters were *Cladium,* Ferns, periphyton, *Peltandra* and *Nymphaea,* detected in 71.5%, 44.7%, 26.5%, 23.1% and 16.8% of the 649 cells respectively

(Table 4, column % Both). The classes that differed more than 5% in presence indicated by either interpreter 1 or 2 were *Peltandra* (10.8%), ferns (10.5%), *Cephalanthus* (5.9%), Periphyton (5.6%) and the 2 *Utricularia* species, *U. foliosa* (5.4%) and *U. purpurea* (5.2%) (Table 4, column % Either) with a mean difference of 3.5% and a standard deviation of 3.2% across all classes. The rarest class detected was *Panicum hemitomon* with a 100% presence agreement in two cells (0.3%), followed by *Pontederia cordata*, identified by only one interpreter in 6 cells (0.9%) and *Persea* ssp. detected in agreement in 2 cells (0.3%) and in 2 additional cells by either interpreter (0.6%) (Table 4, column % Det).

Presence/Absence Morphological Group Profiles

Aggregating all species to their corresponding morphological groups resulted in class agreement (presence and absence) for all 9 morphology groups ranging from 78.1% for herbaceous to 97.8% for tall graminoids and trees, with mean agreement of 93.3% and a standard deviation of 6.2% (Table 5, column % Agree). The most frequently encountered classes with > 20% presence and identified by both interpreters were emergent broadleaf (71.8%), tall graminoid (71.5%), shrub (30.7%), periphyton (26.5%) and floating broadleaf (21.4%) (Table 5, column % Both). The morphological group of herbaceous vegetation had the highest disagreement with 21.9% and a presence agreement of 11%. The other four classes that differed by more than 5% between interpreter were shrub (8.2%), emergent broadleaf (7.7%), floating non-broadleaf or *Utricularia ssp.* (7.6%), and periphyton (5.6%) (Table 5, column % Either). Mean difference for either interpreter was 6.7% with a standard deviation of 6.2% across all classes. The rarest morphological groups recorded were short graminoids, followed by floating non-broadleaf, and trees; these were absent in 91.8%, 85.2% and 85.1% of all cells (Table 5, 100 – (% Either + % Both).

Relative Abundance Species Profiles

Comparing relative abundance estimates of both interpreters indicated that there was a very high agreement in absolute as well as relative percent abundance of all classes. The difference in percent abundance estimates for species across all three interpreted images ranged from less than 0.1% for 4 classes (*Panicum hemitomon, Crinum americanum, Magnolia virginiana, Sagittaria lancifolia*) to greater than 0.5% for *Utricularia purpurea* and periphyton

(both at 0.6%), with the maximum of 1.4% for *Cladium jamaicense* (Table 6, column % Diff). The mean difference was 0.3% with a standard deviation of 0.4%. Abundance estimates of both interpreters for species present > 5% were *Cladium jamaicense* (41.6%), ferns (12.1%), *Salix caroliniana* (6.3%), *Nymphaea odorata* (6.3%), and periphyton (5.6%) (Table 6, column % Mean). Relative abundance difference between interpreters normalized by overall detected abundance of the greater of interpreter 1 or 2 for the same class was largest for *Salix caroliniana* (16.2%), followed by periphyton (10.2%) and *Cladium jamaicense* (3.3%), whereas ferns and *Nymphaea odorata* differed by only 1.6% (Table 6, column % relDiff). The very rare class *Pontederia cordata* was the only class detected by only one interpreter and had therefore a relative difference of 100%.

Relative Abundance Morphological Group Profiles

Relative abundance estimates at aggregated morphological groups ranged from 1% for short graminoids to 41.7% for tall graminoids, represented by only *Cladium jamaicense,* for which the difference in abundance was largest with 1.3% (Table 7, columns % Mean and % Diff). Lowest difference in percent abundance was recorded for floating broadleaf with 0% at 7.1% abundance (Table 7, columns % Mean and % Diff). Mean abundance differences were 0.6% ± 0.5%, whereas the relative abundance difference had a mean of 15% ± 11.5%. The group with the highest relative abundance difference was floating broadleaf with 50% difference (1.6% vs. 0.8%). The relative differences for the groups with presence over 10% were tall graminoid with a difference of 3.1%, followed by emergent broadleaf with 5.1%, and shrub with 9.8% with an overall mean presence of 41.7%, 19.1% and 11.6% respectively.

Site Profiles for Species and Morphological Groups

Site profiles for species and morphological group presence indicated a mean agreement of 95.6% and 93.3% with a minimum agreement of 80.8% and 55.6%, respectively (Table 8). The site differences for relative abundance between species and morphological groups showed similar patterns with a maximum difference in abundance for species corrected for group detection at 62.5% (mean = 11.3%) and for morphological groups 68.8% (mean = 10.1%). The distribution pattern for diversity for both interpreters was very similar (Table 8). Mean diversity

was 3.3 and 3.4 for interpreters 1 and 2, respectively, with a mean difference of 0.3 and a maximum difference of 4 species (Table 8).

Comparison of High- vs. Medium Resolution Photography by Interpreter

A subset of the 100 samples (SRSWR) of the 649 cells interpreted a second time from the 3 cm resolution photographs had a species overlap of 87.5% (14 of 16). One interpreter detected *Cephalanthus occidentalis* and the other *Pontederia cordata.* Detection at the morphological group level had a minor presence discrepancy, interpreter 1 classifying 1/16 of a cell as tree and interpreter 2 detecting 1/16 cells as floating broadleaf, not indicating species. Overall agreement for both interpreters between the lower and higher resolution images when summarized at morphological groups was high with the highest differences observed for Periphyton which decreased by 3.1% and increased by 4.2% for interpreter 2 and 1, respectively. The difference between both interpreters at the higher resolution was 1.1%, whereas the difference in relative abundance increased to 8.4%. The groups that displayed a significant increase in relative abundance for its corresponding species or detection at the group level was emergent broadleaf with an increase of 4.4% and 4.8% and significant decrease was encountered for tall graminoids, which were only detected at the species level (*Cladium jamaicense*) by both interpreters, increasing by 2.5% and 1.8% for interpreters 1 and 2, respectively.

Reduction in detection precision, indicated by an increase in morphological group detection over species recognition, varied for the different morphological groups. Emergent broadleaf and shrub groups were most affected. Classification of emergent broadleaf over corresponding species increased by 19.9% and 36.6% and for shrub 7.1% and 35.41% for interpreters 1 and 2, respectively. Reduction of detection precision, especially for emergent broadleaf species, is explained with the high species detection confidence at the higher resolution. Ferns saw the largest decrease in detection, decreasing by 3.7% and 4.1% for interpreters 1 and 2, respectively. The species that had a consistent increase in detection of relative abundance for both interpreters was *Nymphoides aquatica* and *Cladium jamaicense.*

Discussion

Successful detection of wetland species from high resolution photography acquired by unmanned aerial systems depends in large part on the species morphology, growth density and the resolution and quality of the acquired data. Interpretation of the photographs at the species level needed training but was definitely possible for the majority of species that we included in our species list. We believe that with more training, we could have attempted to distinguish fern species and more tree and shrub species. We felt that additional experience comparing the image in the photograph and the species on the ground would have increased our ability to detect and discriminate. For example, understanding how trees and shrubs differ in color, texture, and overall morphology and branching patterns at different sizes (juvenile vs. adult) would increase discrimination and accuracy in this group. Similarly, additional understanding of how species' images varied between the centers vs. the edge of the photographs (i.e., varying degrees of plan vs. profile views) would increase accuracy of interpretation. The high agreement of visual interpretation results for two interpreters, however, argues that the process is reproducible and can provide exhaustive presence and abundance data for vegetation at a relatively fine taxon scale across large extents and as a permanent record.

The highest agreement for relative abundance was achieved for the morphological group of floating and emergent broadleaf vegetation; more difficulties were encountered for short graminoid species. Detection of floating broadleaf species is easier than emergent vegetation primarily because the leaf surface in relation to the remote sensor view is close to orthogonal, whereas for emergent vegetation, it both has less area and often an oblique or parallel orientation to the sensor view.

Species detection also depends on the timing of image acquisition in relation to species-specific phenological stages. For example, the imagery used in this study was acquired in August, which coincided with the leafless season for the shrub *Cephalanthus occidentalis*. The identification key we used for this species was bright, short and Y-shaped branching features. In this condition, *C. occidentalis* could be confused with sparse *Cladium* but allowed for identification of sub-canopy species. Relative abundance of this species when it is leafed-out (beginning of the wet season) will most certainly increase, while detection of sub-canopy and benthic species will decrease. Consideration of vegetation phenological cycles is valuable for

interpretation and can allow for species-specific detection campaigns during times when the species of interest are least likely to be confused with other vegetation.

In the highest resolution images it was possible to use color, size, and arrangement of flowers and inflorescences to aid in species detection. The small yellow inflorescences of *U. foliosa* were one flag for this species' presence, which could then be confirmed by additional vegetative cues. Similarly, the white/pale purple flowers of *U. purpurea* indicated its presence in thick periphyton mats, as well as in surface water. The large flowers of *Crinum americanum* and *M. virginiana* aided in identification of these species at both levels of resolution. Because flowering intensity varies seasonally for many species, incorporating understanding of flowering phenology into the photo interpreter's determinations can aid in species discrimination. A corollary of this effect is that differences in timing of image acquisition in relation to flowering will also affect detection probability in seasonally flowering species.

The ability to interpret vegetation in the photographs requires training and experience, even for experienced photo interpreters and field botanists. Tree and shrub species, especially, could be hard to distinguish, in part because they are seen from a point-of-view that is very different how they are viewed on the ground. Leaf size, shape, color, and texture, as well as crown shape, provided our main clues, but these may not always distinguish between *Magnolia* and *Ficus*, *Persea* and *Ilex* or even *Salix*. Understanding meso-scale characters, more obvious in these photographs than on the ground or from traditional aerial photography, should allow for more confidence in identification. Potential tree/shrub characters include overall growth form (e.g., compact vs. diffuse), canopy shape (e.g., rounded vs. amorphous), and branching architecture (branching frequency, branch angles) and how these characters interact with leaf arrangement on branches (e.g., clustered vs. evenly distributed) and leaf shape. Training for these characters would require visiting precisely known locations with photographs in hand to correlate the patterns in the image with the species' identifications. Additionally, these types of characters need to be understood for different image resolutions, which provide different details and patterns in the images.

Quality differences between images of medium resolution that were used to compose the mosaic, it was not possible to compare single geo-referenced medium resolution image and mosaic interpretation. Figure 3 demonstrated the quality differences of different sections of the

mosaic. We do not recommend to attempt to detect and identify vegetation at the species or morphological group level from the mosaic, since for different sections of the mosaic the interpretation method needs to be adjusted, which does not allow for a fair comparison and consistent estimation of relative abundances.

For our study the usefulness of the mosaic after referencing to ortho-photography and high accuracy GPS reference locations in the field was limited but essential to the referencing of the single high resolution (~1cm) and medium resolution (~3 cm) individual images. Therefore, we recommend developing a script that allows for batch referencing of each individual image based on automatic reference point extraction from the mosaic. If flight location in combination with attitude and altitude information can be used to improve ground referencing of individual image centers, this process could possibly be automated.

Objective 2: Evaluation of stability and consistency of plant association definitions at multiple sampling intensities derived from continuous hrAP interpreted vegetation data

High resolution aerial photography has the potential to provide data that can address fundamental questions in defining plant associations at different scales. A common practice for deriving species association, assemblage or community classifications is to randomly sample quadrats of a specific size (e.g., 1 m^2), and to detect groups or clusters based on the relative abundance of species in the quadrats using parametric or non-parametric multivariate statistical methods (Greig-Smith 1983, Wildi 2010). When applied to a single sample, this method provides a single solution consisting of groups with associated group labels that does not allow for confidence estimates of generality and consistency of plant association definitions; such estimates, however, are important when attempting to classify new sites (De Cáceres and Wiser 2012). Tichý et al (2011) proposed a bootstrap without replacement sampling framework and comparison of subset partitions to full dataset partitions (Tichý et al. 2011) to evaluate cluster (group) stability. This approach would allow for stability estimation of class definitions for a large dataset but, unless samples are collected for continuous large areas, evaluation for different spatial scales is not supported, since abundance estimates are gathered for a random sample at only one specific grain size. Gathering relative abundance estimates for extended regions in the field to allow for re-sampling at various scales is very time intensive and invasive. The use of relative abundance estimates derived from visually interpreted hrAP as demonstrated in Objective 1 opens up the opportunity to sample across scales and to establish confidence estimates of plant association classification systems at each individual scale. This approach minimizes field sampling to training and verification of visual interpretations and is therefore an economically and environmentally viable option.

For the purpose of investigating stability of single or multi-scale plant association definitions, we developed a re-sampling framework that relies on the existence of spatially continuous vegetation data and allows for sampling and establishment of quantitative plant association definitions from multiple finite samples at various sampling intensities and across multiple scales (Fig. 4). The re-sampling framework to evaluate stability and generality of plant associations considers 3 factors to determine stability. The first addresses variability in optimal

number of plant association clusters derived from k-means cluster analysis across sample sites. The second and third factors address association-specific and location-specific confidence estimates, respectively (Fig. 4). In this framework the classification of plant associations is based on non-hierarchical clustering (i.e., k-means) of relative abundance estimates of plant species. Sampling of relative abundance estimates at the smallest grid size of 2 m generates the highest resolution association definitions, and an iterative re-sampling with subsequent cluster analysis provides multiple plant association definitions (Fig. 4) that, when combined, allow for confidence building on association results from samples. As the sampling area increases, relative abundances of species are aggregated as a weighted average of all neighboring sampling units of the random sample (Fig. 4). The possibility of seamless aggregation of random samples to larger grain sizes enables a multi-scale sampling, and the re-sampling design provides the framework to estimate scale-specific community classification stability and detection probability.

For lack of sufficiently large contiguous interpreted relative abundance estimates at the 2 m grain size, in this study we focused on the effects of sample size on species association pattern detection and confidence building (Fig. 4; red box) rather than on scaling, but the framework was developed for inter-scale analysis as well. The objective of this analysis was to develop methods for vegetation classification using visually interpreted relative abundance data from hrAP and to demonstrate how the use of spatially continuous abundance data derived from hrAP can be useful in the establishment of consistent and stable plant association classification systems when utilized in a re-sampling framework.

Methods

We developed the re-sampling framework in R (R Development Core Team 2013), utilizing several packages in the preparation and post-processing of data as well as in the statistical analysis (Liaw and Wiener 2002, Bivand et al. 2013, Bivand and Lewin-Koh 2013, Oksanen et al. 2013, R Development Core Team 2013). The main parameters that can affect vegetation classification outcome are scale, sample intensity, cluster method and cluster algorithm parameters

. Our framework allows for scale sampling at multiples of the smallest grain size of the raw data input. The sample intensity can be set for user defined ranges and intervals (i.e.

between 50 and 200 samples per cluster analysis, with sample number increasing in intervals of 50). The cluster method we implemented is the k-means cluster algorithm based on the methods of Hartigan and Wong (Hartigan and Wong 1979). Two critical parameters in determining optimal cluster solutions are the number of clusters created and the starting configuration of the clustering process. A criterion to determine the optimal number of clusters is the Calinski-Harabasz criterion, which is an index based on a simple F (ANOVA) statistic evaluating the sum of squares within clusters and among the clusters (Caliński and Harabasz 1974). The cascadeKM function in the vegan R package (Oksanen et al. 2013) implements the Calinski-Harabasz criterion for a range of cluster number solutions between a user-defined minimum (i.e. 2) and maximum (i.e. one third of the number of sampled sites). In order to examine the effect of the starting configuration, for every evaluated cluster size the k-means algorithm was implemented multiple times (i.e. 100) from a random seed. We restricted optimal solutions to cluster results that were represented with at least three representative sites in each cluster. When the optimal number of clusters and cluster solutions were found, all sample sites (649 cells from 3 hrAP images) were assigned to one of the k clusters, and mean presence of all species was calculated for each cluster. Then the cluster name was derived based on the three most abundant species above a user-defined threshold (i.e. 2%).

For each clustering iteration we implemented a supervised classification routine that establishes decision rules based on the relative species distribution of samples assigned to each cluster for the current clustering solution. Classifiers were established based on a recursive partitioning algorithm implemented in a random forest framework, which is founded in the work of Leo Breiman (Breiman 2001, 2002). Random forests minimize bias and avoid over-fitting of single decision tree solutions. When combined, the multiple trees give more robust decision solutions that can provide uncertainty estimates of the final classification tree. The random forest routine of the R package randomForest as implemented by Liaw and Wiener (Liaw and Wiener 2002, Svetnik et al. 2003, Breiman et al. 2006) grows multiple trees from re-sampled (bootstrap) training data subsets (i.e. 500), and, therefore, can generate internal unbiased estimates of the generalization error during the forest construction process (Biau et al. 2008). The final classification decision tree was then applied to the full dataset (i.e., 649 grid cells), predicting plant association membership and association membership probabilities for each

location. The parameters we used to evaluate the plant association classification consistency in the full process of the multi-stage re-sampling process were (1) distribution of optimal number of clusters for all sampling intensities of interest, (2) class-specific model-based error estimates and class-specific classification probabilities of sites that had not been included in the clustering and classifier establishment routine, and (3) spatially explicit (site-specific) distribution of mean and standard deviation of membership probability and consistency of plant association label assignment.

We applied this analysis framework to evaluate the effect of sample size on consistency of class-specific and site-specific probability estimates in the three high resolution images from WCA 3A WEST that we had visually interpreted from the hrAP (Objective 1, above).

Results

The number of optimal vegetation clusters ranged from 4 to 10 with a mean of 4.5 ±1.2 (mean ± SD) for sample size 50, declining to 4.1 ± 0.4 for 200 samples. The mean diversity of final clusters increased from 8.8 ± 1.3 species to 12.6 ± 1.1, 13.9 ± 1.1 and 15.0 ± 1.1 for sample sizes 50, 100, 150 and 200, respectively. Model-based classification error for the random forest classifiers decreased from 12.2 ± 8.3 for 50 samples to 7.2 ± 3.4, 5.9 ± 2.6 and 5.8 ± 2.3 for sample intensities 100, 150 and 200, respectively.

Plant association frequencies and probabilities were derived from cluster results across all iterations. The most frequently detected plant association across all sampling intensities was the *Cladium-Fern-Peltandra* association, which was encountered in 306 of the 400 cluster iteration results (76.5%), followed by the *Nymphaea-Periphyton-Cladium (*40%), *Fern-Salix-Cephalanthus* (18.5%), *Nymphaea-Periphyton-Utricularia* (18.0%), and *Salix-Fern-Cladium* (18.5%). The most abundant tree association that was detected was *Magnolia-Myrica-Cladium,* represented in 11% of the cluster results across all iterations. More than 95% of all cells were assigned to 5 associations for 50 and 100 samples and to 3 associations for 150 and 200 samples.

Association assignment probabilities based on the highest probability across all 100 iterations and by 4 sampling intensities indicated that the *Cladium-Fern-Peltandra* association was detected not only at the highest frequency but also with the highest average probability of 0.82, 0.88, 0.90 and 0.92 for 50, 100, 150 and 200 samples, respectively (Table 9). Both cluster

distribution and associated probabilities from the 100 sample cluster iteration are mapped for each hrAP image in Figs. 5-7. The four association groups that were across all four sampling intensities were *Magnolia-Cladium-Myrica* was assigned mean probabilities of 0.66 (50 samples), 0.60 (100 samples), 0.86 (150 samples), and 0.91 (200 samples). *Nymphaea-Periphyton-Cladium* was detected with the second highest average probability at 50 samples with a probability of 0.74; it was 4th at 100 samples with 0.81 (Figs. 5-7) and 3rd at 150 and 200 at probabilities of 0.83 and 0.88, respectively. The *Fern-Salix-Cephalanthus* association had a mean probability of 0.84, 0.83, 0.72 and less than 0.65 for 200, 150, 100 and 50 respectively (Table 9).

Site specific post-classification association assignment probabilities summarized across all 649 cells ranged from 0.78 ± 0.14, 0.84 ± 0.12, 0.87 ± 0.11, and 0.89 ± 0.1 for 50, 100 (Figs. 5-7), 150 and 200 samples, respectively. The combination of frequency and probability provide a better understanding for cluster representativeness and stability for the evaluated region. For example, for a sampling intensity of 100 samples the 5 most frequently encountered associations were *Cladium-Fern-Peltandra* (63%) with a probability of 0.88, *Nymphaea-Periphyton-Cladium* (11%) with a probability of 0.81, *Salix-Fern-Cladium* (9%) and *Fern-Salix-Cephalanthus* (8%) with probabilities of 0.83, and *Magnolia-Myrica-Cladium* (4%) with a probability of 0.60 (Figs. 5-7).

Discussion

The hrAP is extremely useful for deriving plant association classifications because it enables estimation of class- and site-specific membership probability distributions and their associated parameters. Confidence building and stability assessment of plant associations derived from samples is needed when attempting to detect associations from remotely sensed data. The application of association classifications to larger areas or entire regions is only valid if stability and consistency are confirmed. The use of hrAP allows for instantaneous visual feedback on adequacy of associations that results from cluster analysis. Multivariate statistical methods (i.e., clustering) have a tendency to provide multiple statistically reasonable solutions that can be highly variable but are caused by minor differences in parameter selection (parameter sensitive). The re-sampling framework we developed enables visual and statistical evaluation of

plant associations before they are used in detection and mapping applications. Based on visual validation of association classifications over a relatively large area (all combined visually interpreted photographs), clustering parameters can be adjusted until statistically valid and visually reasonable assignments for each grid cell are achieved. Visual evaluation of results coupled with statistical support allowed us to make the decision to select sub-optimal statistical solutions that had a more appealing association classification schema, decreasing site-specific mean probability of association assignment by only 2%.

The generality and spatial extensibility of a locally derived association classification can be verified for areas that extend beyond the sampled area (larger or more distant) if relative abundance estimates exist at the grain size at which association classifications were derived. In this study we demonstrated the value of the use of hrAP-derived abundance estimates in a spatially explicit form, but the validity of the results is limited at this time, since the sample size for re-sampling procedures needs to be larger. At the 200 sample intensity, almost 1/3 of all cells were selected in every sample draw, which means that there was a great overlap of the sample sets and thus solutions naturally converge. A second aspect of limited spatial extent is spatial auto-correlation of samples, which is not necessarily a crucial aspect, because variability of species co-occurrence over short distances is very high in our study environment. Because of the lack of a sufficiently large contiguous area of the highest resolution photographs, we could not evaluate the framework for multi-scale applications. Once larger regions are available and visually interpreted, additional spatial restrictions could be applied during each sampling procedure.

Several of our clustering framework parameters need to be revisited and adjusted. One of these is the minimum number of classes that are expected as sampling intensity increases. The decrease in optimal number of clusters based on within and between cluster variances (the Calinski-Harabasz criterion) might not be the most useful criterion, especially if cluster sizes are expected to differ as much as they do in the case of our study area. Optimization of cluster count is based on the minimal number of supported cluster solutions excluding single species associations. At the 2 m grain size, pure classes need to be permitted, especially for large tree species. As the geographic extent and grain size increase, the set of current parameters might be more appropriate.

Tables and Figures

Table 1 Number of raw images, mean altitudes and standard deviations in meters above ground (mag) acquired at low and high flight altitudes cross-tabulated by study area.

	Low Altitude	High Altitude
East number of Images	97	931
West number of Images	91	1063
Mean Altitude (mag)	35.7	136.1
Standard Deviation (mag)	8.4	11.8

Table 2 Camera specifications and raw and geo-referenced image characteristics.

Camera Type	Dimension	Value	Units	Image Name	Flight Altitude (mag)	Nominal Ground Resolution (cm)	2nd Order Polynomial RMSE (cm)	Number of Reference Points	Spatial Reference Resolution (cm)
Olympus E420	sensorWidth	17.3	mm	20120816222532_513	33.7	0.64	16.7	10	1.06
	sensorHeight	13	mm	20120815030421_285	128.6	2.44	15.1	46	3.15
	resWidth	3648	dpi	20120816222532_557	34.2	0.65	12.8	58	1.09
	resHeight	2736	dpi	20120814230041_255	128.2	2.43	26	78	3.07
	cropFactor	2.02	-	20120816222532_550	32.2	0.61	28.5	54	1.03
	focalLength	25	mm	20120814230041_719	133.5	2.53	28.5	184	3.1

Table 3 Vegetation classes considered in the visual interpretation process. *BOLD CAPITALS* indicate morphological groups. *CAPTIALS* indicate sub-group.

Vegetation Classes			
FLOATING BROADLEAF	***EMERGENT BROADLEAF***	***SHORT GRAMINOID***	***SHRUB***
Nymphaea odorata	*FERN*	*Panicum hemitomon*	*Salix caroliniana*
Nymphoides aquatica	*Acrostichum danaeifolium*	*Rhynchospora tracyi*	*Myrica cerifera*
Nuphar advena	*Peltandra virginica*	*Rhynchospora inundata*	*Chrysobalanus icaco*
	Crinum americanum	*Eleocharis ssp.*	*Cephalanthus occidentalis*
FLOATING NON-BROADLEAF	*Sagittaria lancifolia*		
Utricularia foliosa	*Pontederia cordata*	***TALL GRAMINOID***	***TREE***
Utricularia purpurea	*Thalia geniculata*	*Cladium jamaicense*	*Annona glabra*
		Typha domingensis	*Magnolia virginiana*
PERIPHYTON	***HERBACEOUS***		*Ilex cassine*
			Persea ssp.
			Ficus ssp.

Table 4 Species profile for presence/absence data from two photointerpreters (Int 1 and Int 2). % Agree = percent that both interpreters identified a class as present; % Int 1, % Int 2 are the percent of all cells in which Int 1 or Int 2 identified a class as present; % Both is the percent of all cells in which both interpreters identified a class as present; % Either is the percent of all cells in which either interpreter identified a class as present; % Det = the percent of all cells in which a class was determined to be present by at least one interpreter.

Vegetation Class	% Agree	% Int 1	% Int 2	% Both	% Either	% Det
Nymphaea odorata	97.7	1.7	0.6	16.8	2.3	19.1
Nymphoides aquatica	96.8	2.6	0.6	8.5	3.2	11.7
Utricularia foliosa	94.6	4.0	1.4	4.3	5.4	9.7
Utricularia purpurea	94.8	4.8	0.5	4.2	5.2	9.4
FERN	89.5	3.5	6.9	44.7	10.5	55.2
Peltandra virginica	89.2	7.7	3.1	23.1	10.8	33.9
Crinum americanum	97.2	1.5	1.2	7.7	2.8	10.5
Sagittaria lancifolia	97.8	1.5	0.6	2.0	2.2	4.2
Pontederia cordata	99.1	0.9	0.0	0.0	0.9	0.9
Panicum hemitomon	100.0	0.0	0.0	0.3	0.0	0.3
Cladium jamaicense	97.8	0.8	1.4	71.5	2.2	73.7
Salix caroliniana	95.4	3.7	0.9	15.9	4.6	20.5
Myrica cerifera	98.2	0.5	1.4	4.3	1.9	6.2
Chrysobalanus icaco	99.7	0.0	0.3	0.9	0.3	1.2
Cephalanthus occidentalis	94.1	3.2	2.6	11.6	5.9	17.4
Annona glabra	99.2	0.5	0.3	5.9	0.8	6.6
Magnolia virginiana	99.1	0.5	0.5	6.6	0.9	7.6
Persea ssp.	99.4	0.3	0.3	0.3	0.6	0.9
PERIPHYTON	94.5	1.9	3.7	26.5	5.6	32.1

Table 5 Morphological group profile for presence/absence data from two photointerpreters (Int 1 and Int 2). % Agree = percent that both interpreters identified a class as present; % Int 1, % Int 2 are the percent of all cells in which Int 1 or Int 2 identified a class as present; % Both is the percent of all cells in which both interpreters identified a class as present; % Either is the percent of all cells in which either interpreter identified a class as present; % Det = the percent of all cells in which a class was determined to be present by at least one interpreter.

Vegetation Class	% Agree	% Int 1	% Int 2	% Both	% Either	% Det
FLOATING BROADLEAF	97.4	1.9	0.8	21.4	2.6	24.0
FLOATING NON-BROADLEAF	92.5	6.3	1.2	7.2	7.6	14.8
EMERGENT BROADLEAF	92.3	1.9	5.9	71.8	7.7	79.5
SHORT GRAMINOID	97.1	2.0	0.9	5.2	2.9	8.2
TALL GRAMINOID	97.8	0.8	1.4	71.5	2.2	73.7
HERBACEOUS	78.1	6.2	15.7	11.1	21.9	33.0
SHRUB	91.8	4.9	3.2	30.7	8.2	38.8
TREE	97.8	0.9	1.2	12.8	2.2	15.0
PERIPHYTON	94.5	1.9	3.7	26.5	5.6	32.1

Table 6 Species profiles for relative abundance estimates of vegetation classperformed by two interpreters in percent of 649 grid cells. Vegetation Class as in Table 3. % Int 1 and % Int 2 = percent class was found by each interpreter; % Mean = mean of % Int 1 and % Int 2. %Diff is absolute percent difference between interpreter 1 (Int 1) and interpreter (Int 2). Relative difference (%relDiff) is the difference normalized by the maximum relative abundance estimated by either interpreter 1 or 2. * indicates species that was detected by both interpreters at percentages less than 0.1% but in full agreement (0% difference).

Vegetation Class	% Int 1	% Int 2	% Mean	% Diff	% relDiff
FLOATING BROADLEAF	0.0	0.0	0.0	0.0	-
Nymphaea odorata	6.2	6.3	6.3	0.1	1.6
Nymphoides aquatica	0.9	0.8	0.9	0.1	11.1
Utricularia foliosa	0.6	0.4	0.5	0.2	33.3
Utricularia purpurea	1.0	0.4	0.7	0.6	60.0
EMERGENT BROADLEAF	1.0	2.2	1.6	1.2	54.5
FERN	12.0	12.2	12.1	0.2	1.6
Peltandra virginica	4.1	3.8	4.0	0.3	7.3
Crinum americanum	1.1	1.1	1.1	0.0	0.0
Sagittaria lancifolia	0.4	0.4	0.4	0.0	0.0
Pontederia cordata	0.1	0.0	0.1	0.1	100.0
SHORT GRAMINOID	0.8	1.0	0.9	0.2	20.0
*Panicum hemitomon **	0.0	0.0	0.0	0.0	0.0
TALL GRAMINOID	0.0	0.1	0.1	0.1	100.0
Cladium jamaicense	42.3	40.9	41.6	1.4	3.3
HERBACEOUS	2.1	2.4	2.3	0.3	12.5
SHRUB	0.6	0.7	0.7	0.1	14.3
Salix caroliniana	6.8	5.7	6.3	1.1	16.2
Myrica cerifera	1.0	1.1	1.1	0.1	9.1
Chrysobalanus icaco	0.2	0.3	0.3	0.1	33.3
Cephalanthus occidentalis	3.5	3.1	3.3	0.4	11.4
TREE	0.1	0.1	0.1	0.0	0.0
Annona glabra	2.6	2.3	2.5	0.3	11.5
Magnolia virginiana	4.3	4.3	4.3	0.0	0.0
Persea ssp.	0.1	0.2	0.2	0.1	50.0
PERIPHYTON	5.9	5.3	5.6	0.6	10.2

Table 7 Morphological group profiles for relative abundance estimates performed by two interpreters in percent of 649 grid cells. Vegetation Class as for morphological classes in Table 3. % Int 1 and % Int 2 = percent class was found by each interpreter; % Mean = mean of % Int 1 and % Int 2. %Diff is absolute percent difference between interpreter 1 (Int 1) and interpreter (Int 2). Relative difference (%relDiff) is the difference normalized by the maximum relative abundance estimated by either interpreter 1 or 2.

Vegetation Class	% Int 1	% Int 2	% Mean	% Diff	% relDiff
FLOATING BROADLEAF	7.1	7.1	7.1	0.00	0.0
FLOATING NON-BROADLEAF	1.6	0.8	1.2	0.80	50.0
EMERGENT BROADLEAF	18.6	19.6	19.1	1.00	5.1
SHORT GRAMINOID	0.9	1	1.0	0.10	10.0
TALL GRAMINOID	42.3	41	41.7	1.30	3.1
HERBACEOUS	2.1	2.4	2.3	0.30	12.5
SHRUB	12.2	11	11.6	1.20	9.8
TREE	7.1	6.9	7.0	0.20	2.8
PERIPHYTON	5.9	5.3	5.6	0.60	10.2

Table 8 Site profile summary of vegetation class relative abundance differences between two interpreters and corrected differences for species (relAbn SpecDif, relAbn SpecDifCor) and for morphological group (relAbn MorphDif); of vegetation class presence/absence agreement between two interpreters for species (Pres/Abs SpecAgree) and morphological group (Pres/Abs. MorphAgree); and diversity per cell for each interpreter (Diversity Int1, Diversity Int2), as well as diversity difference per cell between Int1 and Int2 (Diversity Dif). Data for 649 sites (cells) in 3 hrAP.

	Min.	1st Qu.	Median	Mean	3rd Qu.	Max.
relAbn SpecDif	0.0	6.3	12.5	12.6	18.8	68.8
relAbn SpecDifCor	0.0	6.3	9.4	11.3	15.6	62.5
relAbn MorphDif	0.0	3.1	9.4	10.1	15.6	68.8
Pres/Abs SpecAgree	80.8	92.3	96.2	95.6	100.0	100.0
Pres/Abs. MorphAgree	55.6	88.9	100.0	93.3	100.0	100.0
Diversity Int1	1.0	2.0	3.0	3.3	4.0	9.0
Diversity Int2	1.0	2.0	3.0	3.4	4.0	10.0
Diversity Dif	0.0	0.0	0.0	0.3	0.0	4.0

Table 9 Mean association assignment probability (Mn Prob) of the four most frequently occurring plant associations for the 50, 100, 150 and 200 sampling intensities.

Plant Association	Mn Prob (50)	Mn Prob (100)	Mn Prob (150)	Mn Prob (200)
Cladium-Fern-Peltandra	0.82	0.88	0.9	0.92
Magnolia-Cladium-Myrica	0.66	0.6	0.86	0.91
Nymphaea-Periphyton-Cladium	0.74	0.81	0.83	0.88
Fern-Salix-Cephalanthus	0.84	0.83	0.73	0.65

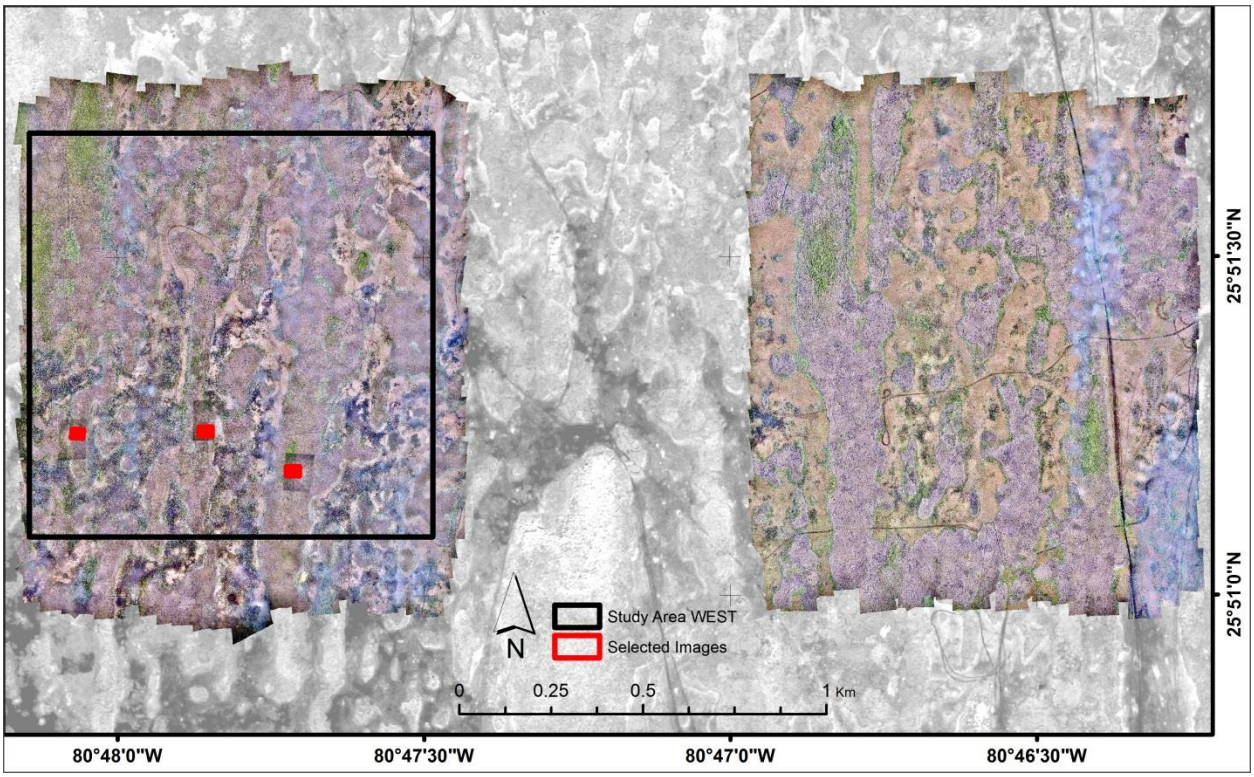

Figure 1 Aerial mosaic of regions 'WEST' and 'EAST'. Red rectangles in study area 'WEST' indicate locations of the three selected highest resolution images that were visually interpreted; these same areas were also visually interpreted for the medium resolution images.

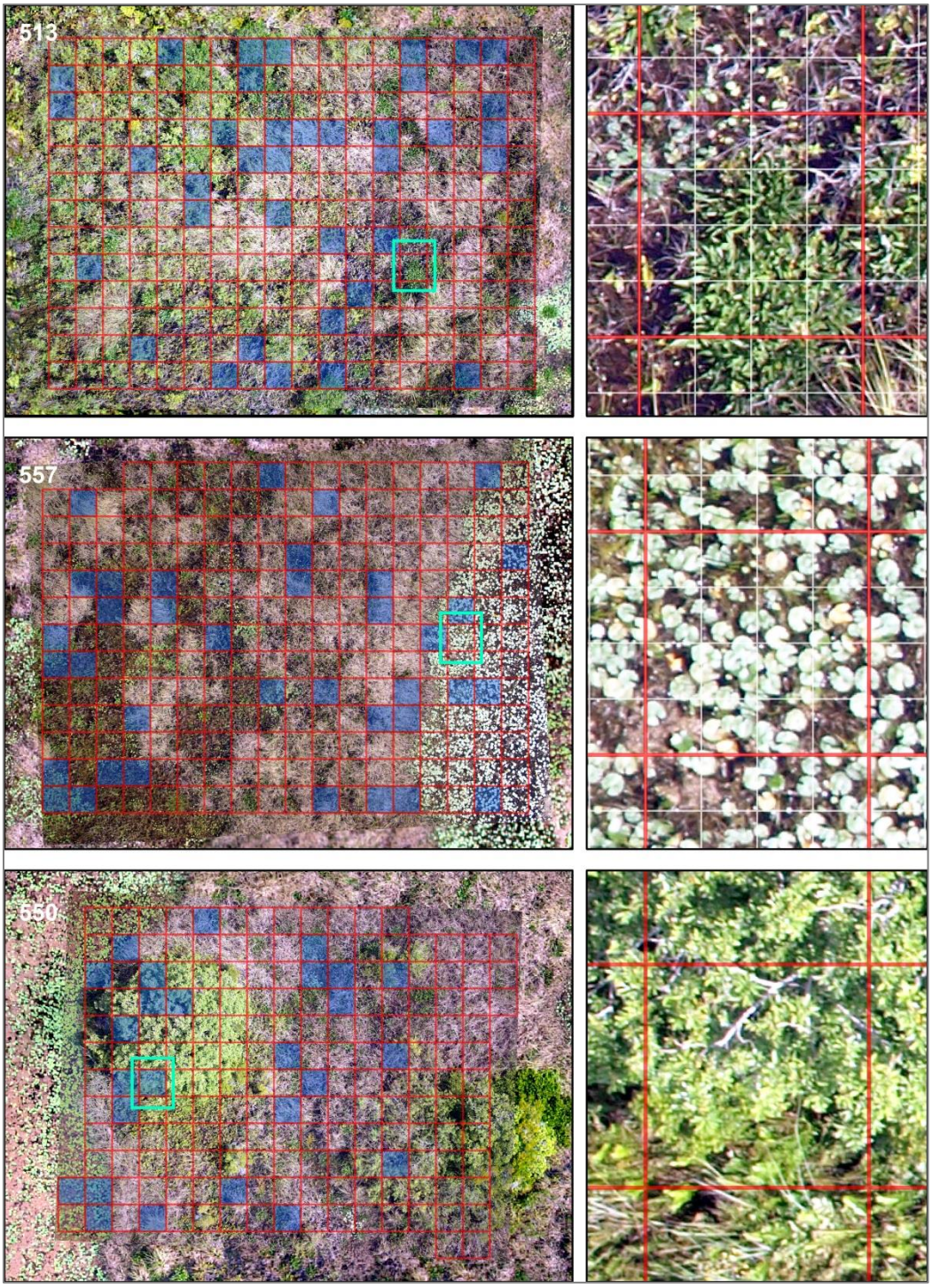

Figure 2 Top to bottom: 1 cm resolution geo-referenced aerial photographs 513, 557 and 550. The right panels show 1:50 zoom areas; these locations are outlined in turquois in the overview maps to the left. Red rectangles are the 2 x 2 m grid; the blue transparent cells in images on the left indicate the 100 samples that were also interpreted at the 3 cm image resolution. Top right: Cell with about 44% *Peltandra virginica*; 12.5% *Nymphaea odorata*, periphyton and *Cephalanthus occidentalis*; and 6% *Nymphoides aquatica* and herbaceous vegetation. Center right: 75% *Nymphaea odorata*; 18.25% periphyton and short graminoids. Bottom right: 75% *Magnolia virginica*; 12% ferns; and 6% periphyton and *Myrica cerifera*.

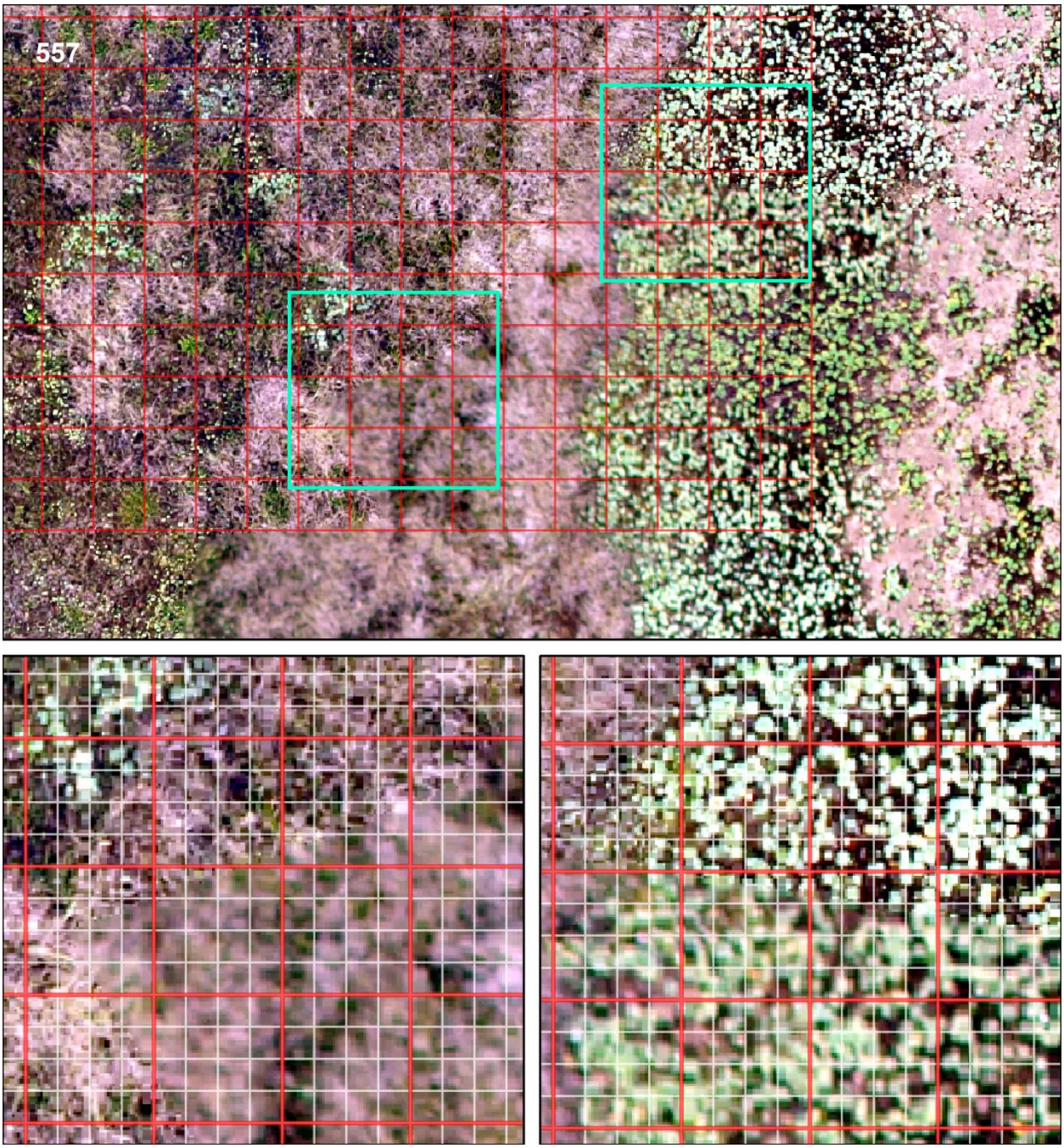

Figure 3 Quality differences across the 3 cm mosaic for a *Cladium jamaicense* and *Nymphaea odorata* environment within the boundaries of image 557.

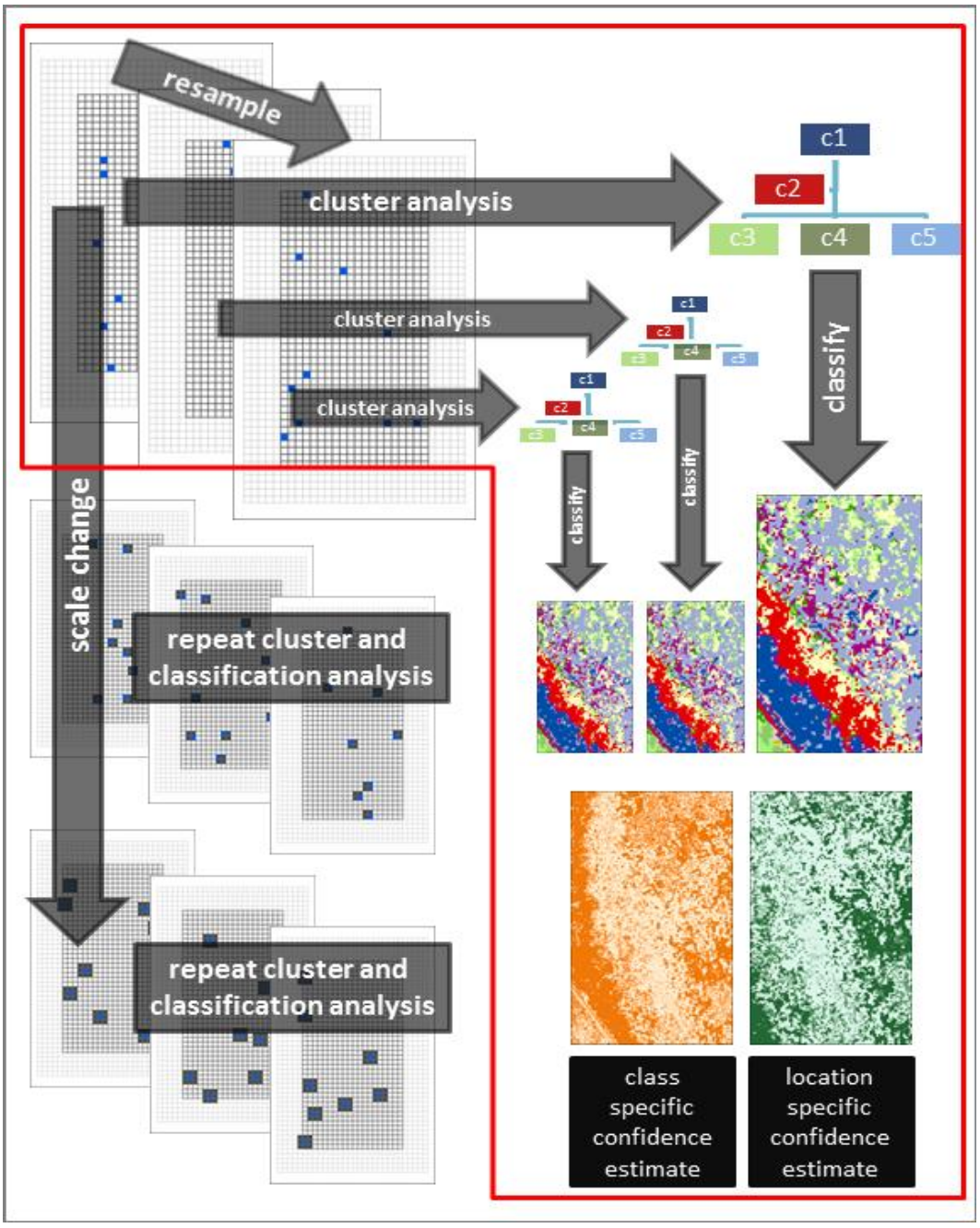

Figure 4 Schema of resampling framework to evaluate plant association stability. The framework allows for plant association-specific as well as location-specific confidence estimates at various spatial scales. Each of the grid cells has visually interpreted relative vegetation abundance estimates at the species or morphological growth form level associated to it. Re-sampling at the minimum mapping unit level and subsequent application of cluster algorithms generates multiple plant association definitions and labels at the highest resolution. We evaluated sampling intensities at the smallest grain size (interpretation scale) of 2 m. For each of the four sampling intensities (50, 100, 150 and 200) we re-sampled 100 times from all 649 grid cells. For each random sample we established clusters using the Hartigan-Wong k-means clustering method. Each sample was assigned to a cluster and mean species abundance was calculated. Classification tree classifiers were generated for each cluster result using a random forest algorithm (500 trees per iteration). Model-based classification errors across all iterations provide class-specific confidence estimates. All 649 grid cells were classified with each classifier, which resulted in location-specific confidence estimates of association probability.

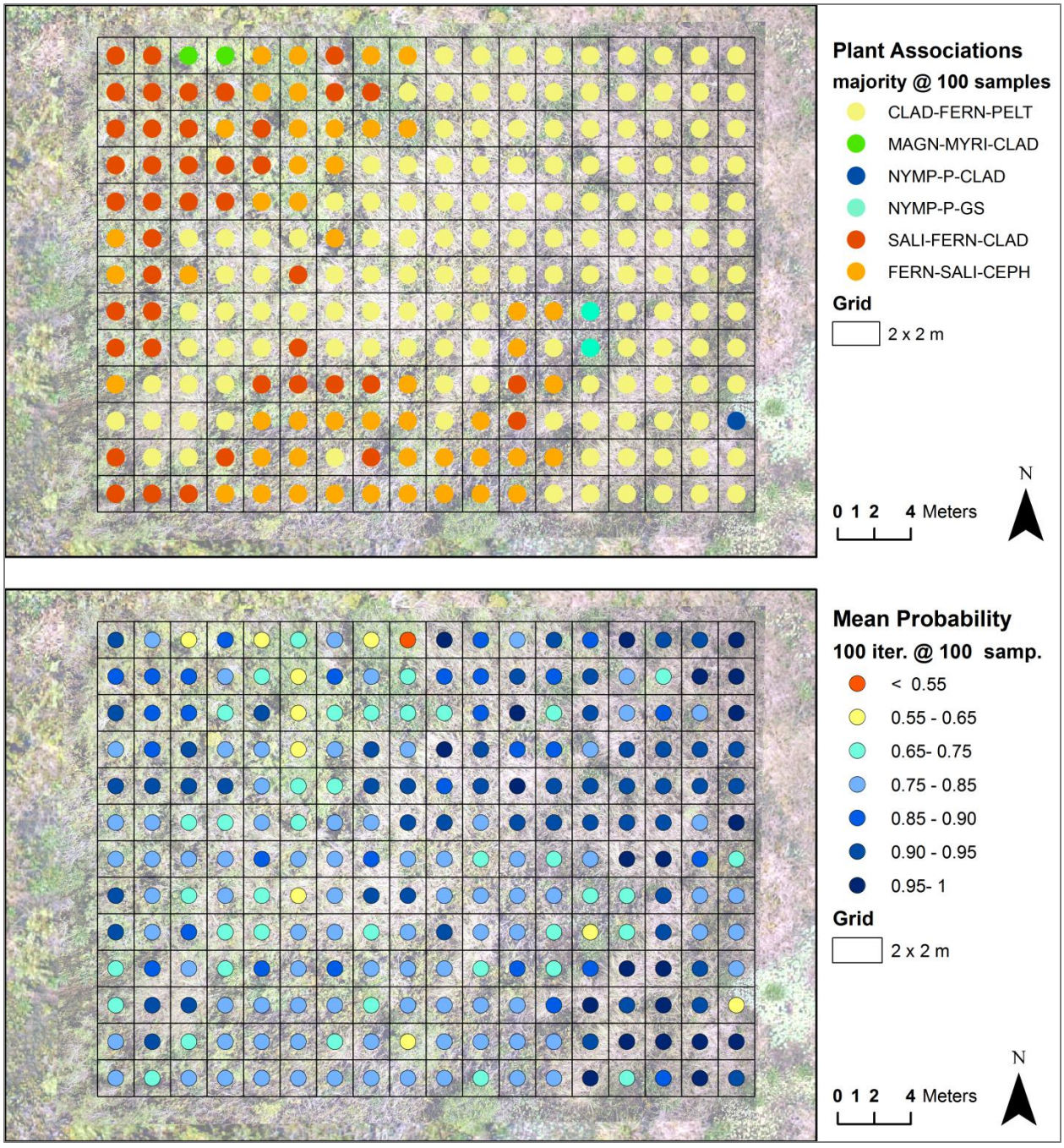

Figure 5 Plant associations and mean probability estimates for image 513. Plant associations were derived from 100 cluster and classification iterations based on a sampling intensity of 100 samples per iteration (top panel). Location-specific mean probabilities for assigned plant association labels were determined from the 100 iterations (bottom panel). CLAD-FERN-PELT = *Cladium-Fern-Peltandra* class; MAGN-MYRI-CLAD = *Magnolia-Myrica-Cladium* class; NYMP-P-CLAD = *Nymphaea-Periphyton-Cladium* class; NYMP-P-GS = *Nymphaea-Periphyton-Graminoid Short* class; SALI-FERN-CLAD = *Salix-Fern-Cladium* class; FERN-SALI-CEPH = *Fern-Salix-Cephalanthus* class.

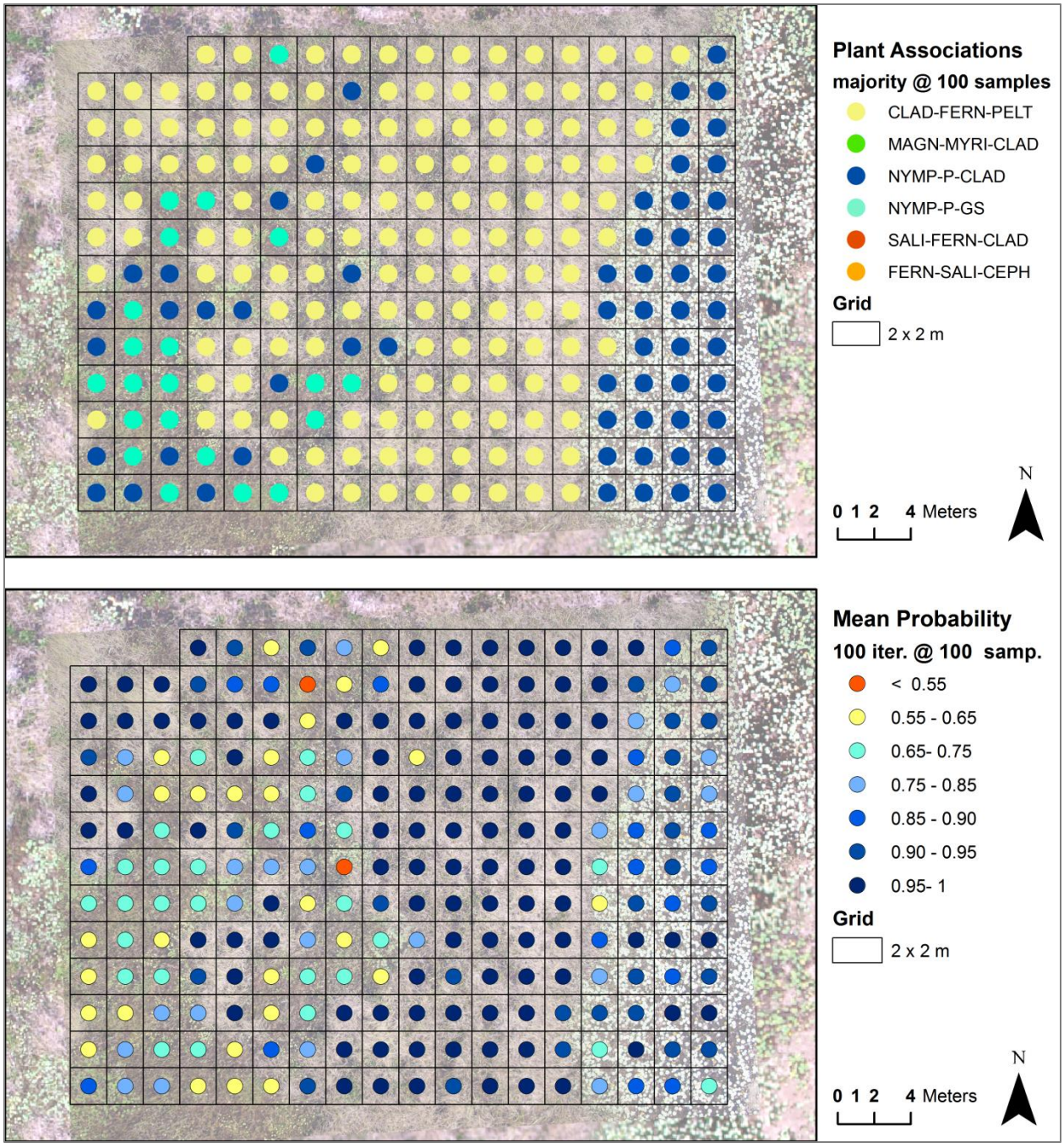

Figure 6 Plant associations and mean probability estimates for image 557. Plant associations were derived from 100 cluster and classification iterations based on a sampling intensity of 100 samples per iteration (top panel Location-specific mean probabilities for assigned plant association labels were determined from the 100 iterations (bottom panel). Legend abbreviations as in Figure 5.

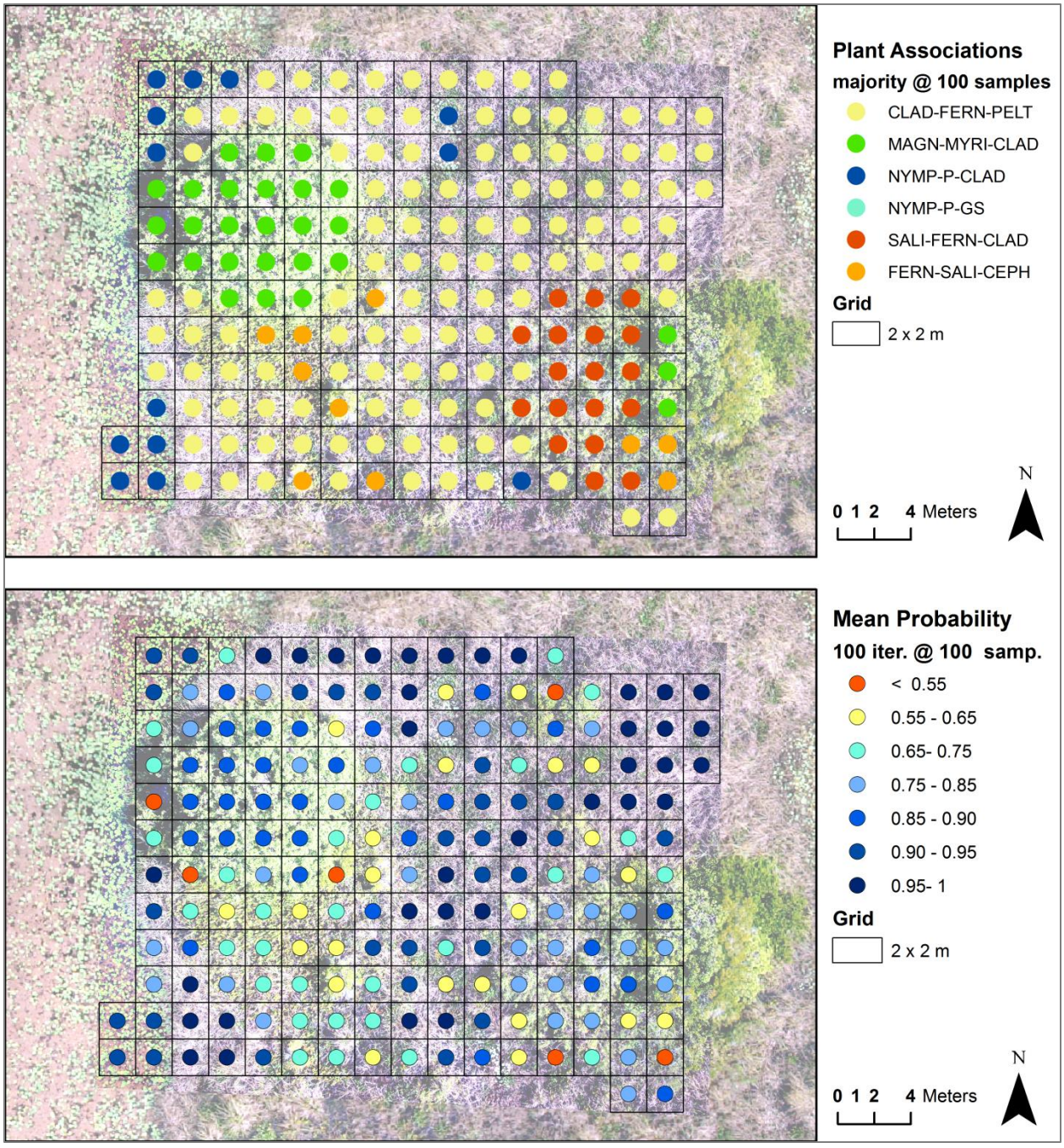

Figure 7 Plant associations and mean probability estimates for image 550. Plant associations were derived from 100 cluster and classification iterations based on a sampling intensity of 100 samples per iteration (top panel). Location-specific mean probabilities for assigned plant association labels were determined from the 100 iterations (bottom panel). Legend abbreviations as in Figure 5.

References

Biau, G., L. Devroye, and G. Lugosi. 2008. Consistency of Random Forests and Other Averaging Classifiers. J. Mach. Learn. Res. **9**:2015-2033.

Bivand, R., T. Keitt, and B. Rowlingson. 2013. rgdal: Bindings for the Geospatial Data Abstraction Library.

Bivand, R. and N. Lewin-Koh. 2013. maptools: Tools for reading and handling spatial objects.

Breiman, L. 2001. Random Forests. Mach. Learn. **45**:5-32.

Breiman, L. 2002. Manual On Setting Up, Using, And Understanding Random Forests V3.1.

Breiman, L., A. Cutler, A. Liaw, and M. Wiener. 2006.

Caliński, T. and J. Harabasz. 1974. A dendrite method for cluster analysis. Communications in Statistics **3**:1-27.

De Cáceres, M. and S. K. Wiser. 2012. Towards consistency in vegetation classification. Journal of Vegetation Science **23**:387-393.

Francis, J. M. and J. M. Klopatek. 2000. Multiscale Effects of Grain Size on Landscape Pattern Analysis. Annals of GIS **6**:27 - 37.

Gann, D., J. H. Richards, and H. Biswas. 2012. Determine the effectiveness of vegetation classification using WorldView 2 satellite data for the Greater Everglades. South Florida Water Management District, West Palm Beach, FL.

Greig-Smith, P. 1983. Quantitative plant ecology. 3 edition. University of California Press, Berkeley.

Hartigan, J. A. and M. A. Wong. 1979. Algorithm AS 136: A K-Means Clustering Algorithm. Journal of the Royal Statistical Society. Series C (Applied Statistics) **28**:100-108.

Lam, N. S.-N. and D. A. Quattrochi. 1992. On the Issues of Scale, Resolution, and Fractal Analysis in the Mapping Sciences. The Professional Geographer **44**:88 - 98.

Liaw, A. and M. Wiener. 2002. Classification and Regression by randomForest. R News **2**:18-22.

Marignani, M., E. Del Vico, and S. Maccherini. 2007. Spatial scale and sampling size affect the concordance between remotely sensed information and plant community discrimination in restoration monitoring. Biodiversity and Conservation **16**:3851-3861.

Mas, J.-F., Y. Gao, and J. A. N. Pacheco. 2010. Sensitivity of landscape pattern metrics to classification approaches. Forest Ecology and Management **259**:1215-1224.

O'Neill, R. V., J. R. Krummel, R. H. Gardner, G. Sugihara, B. Jackson, D. L. DeAngelis, B. T. Milne, M. G. Turner , B. Zygmunt, S. W. Christensen, V. H. Dale, and R. L. Graham. 1988. Indices of landscape pattern. Landscape Ecology **1**:153-162.

Oksanen, J., F. G. Blanchet, R. Kindt, P. Legendre, P. R. Minchin, R. B. O'Hara, G. L. Simpson, P. Solymos, M. Henry, H. Stevens, and H. Wagner. 2013. vegan: Community Ecology Package.

Ostapowicz, K., P. Vogt, K. Riitters, J. Kozak, and C. Estreguil. 2008. Impact of scale on morphological spatial pattern of forest. Landscape Ecology **23**:1107-1117.

R Development Core Team. 2013. R: A Language and Environment for Statistical Computing. R Foundation for Statistical Computing, Vienna, AT.

Rocchini, D. 2007. Effects of spatial and spectral resolution in estimating ecosystem [alpha]-diversity by satellite imagery. Remote Sensing of Environment **111**:423-434.

Schlup, B. M. and H. H. Wagner. 2008. Effects of study design and analysis on the spatial community structure detected by multiscale ordination. Journal of Vegetation Science **19**:621-632.

Svetnik, V., A. Liaw, C. Tong, J. Culberson, R. Sheridan, and B. Feuston. 2003. Random Forest: A Classification and Regression Tool for Compound Classification and QSAR Modeling. Journal of Chemical Information and Computer Sciences **43**:1947 - 1958.

Tichý, L., M. Chytrý, and P. Šmarda. 2011. Evaluating the stability of the classification of community data. Ecography **34**:807-813.

Tischendorf, L. 2001. Can landscape indices predict ecological processes consistently? Landscape Ecology **16**:235-254.

Turner, M. G. 1989. Landscape Ecology: The Effect of Pattern on Process. Annual Review of Ecology and Systematics **20**:171-197.

Wildi, O. 2010. Data Analysis in Vegetation Ecology. Wiley-Blackwell, Oxford.

Wu, J. 1999. Hierarchy and scaling : Extrapolating information along a scaling ladder. Canadian Aeronautics and Space Institute, Ottawa, ON, CANADA.

Wu, J. 2004. Effects of changing scale on landscape pattern analysis: scaling relations. Landscape Ecology **19**:125-138.